福井大学リポジトリ
UNIVERSITY OF FUKUI
REPOSITORY

Voltammetric potentials of polyaniline varying with electric percolation

メタデータ	言語: English 出版者: 公開日: 2011-05-10 キーワード (Ja): キーワード (En): 作成者: CHEN, Han, AOKI, Koichi, KAWAGUCHI, Fumihiko, CHEN, Jingyuan, NISHIUMI, Toyohiko メールアドレス: 所属:
URL	http://hdl.handle.net/10098/3205

Voltammetric potentials of polyaniline varying with electric percolation

Han Chen, Koichi Aoki*, Fumihiko Kawaguchi, Jingyuan Chen, Toyohiko Nishiumi

Department of Applied Physics, University of Fukui

3-9-1 Bunkyo, Fukui, 910-8507 Japan

Abstract

The reduction of the emeraldine form of polyaniline film into leucoemeraldine, which corresponds to the conversion of an electric conductor into an insulator, shifted in the positive direction with increasing scan rate and film thickness. Similar dependence was found in the diffusion-controlled voltammograms of dispersed polyaniline latex particles with eight diameters ranging from 0.2 to 7.5 μm. The particles were synthesized by coating dispersed polystyrene latex with polyaniline. These variations were explained in terms of electric percolation of the conducting species to the electrode. The theoretical expression for the Nernst equation was derived on the assumption that the percolated and the un-percolated conducting species took inner potentials of the electrode and the solution phase, respectively. The conducting species does not participate in the determination of the equilibrium potential, though it participates in the Faradaic current. The cathodic peak potential shifted in the negative direction with an increase in particle size, solution viscosity, and film thickness, as predicted from the derived Nernst equation.

keywords: polyaniline films; electric percolation; Nernst equation; latex suspensions; conducting species.

* phone +81 090 8095 1906, fax +81 776 27 8750, e-mail kaoki@u-fukui.ac.jp

1. Introduction

Polyaniline (PANI), an electrically conducting polymer, exhibits three redox states in acidic solution: the reduced state of leucoemeraldine, the electrically conducting half-oxidized state of emeraldine, and the insulating oxidized state of pernigraniline [1,2]. The redox reaction between the first and the second states is reversible and reproducible, whereas pernigraniline is chemically unstable and deteriorates the electrochemical activity [3-6]. Therefore, most of iterative redox conversion occurs between leucoemeraldine and emeraldine. A typical voltammogram of this conversion in electrochemically polymerized PANI films, shown in Fig. 1(a), has a sharp anodic peak and a broad cathodic wave with a tail. They are asymmetric in voltammetric shape, with large differences in the peak potentials. This asymmetry is a central theme in the characterization of conducting polymers [7- 13]. Asymmetric conversion has also been found in electrochemical ESR signals [14], spectro-electrochemical responses [15], conductivity vs. potential curves [16,17], beam deflection [18], radiotracer analysis [19], electrochemical quartz crystal microbalance [20], and acoustic measurements [21]. Asymmetry is revealed to current-time curves [22,23]. Asymmetry may be caused by the structure change between local and extended polymer motions [11], the mechanical work coupled with the redox reaction [13], the propagation of the conducting zone [24,25], the logarithmic relaxation [26], and/or the structural rearrangement of polyaniline during the redox reaction [12].

Although several causes of asymmetry have been recognized, they have not been quantitatively confirmed yet to our knowledge. Most of them are explained intuitively by the blocking of the redox reaction decreasing the current. However, they fail to interpret the large difference between the anodic and the cathodic peak potentials. The peak potentials represent the equilibrium between leucoemeraldine and emeraldine [1], including hydrogen ion participation [27] and complications from redox interactions [28]. Unfortunately, these contributions do not contain any explicit information about the structural change during the

redox reaction. It is necessary to consider the electrode potentials associated with the structural change.

When the conducting species of polyaniline is connected electrically to the electrode, called electrical percolation, it should take the inner potential of the electrode rather than the solution phase. Consequently, the Nernst equation does not express the relation between the electrode potential and the concentration of the conducting species. In contrast, the conducting species without any electrode connection takes the inner potential of solution, and the conventional Nernst equation holds. Therefore, the observed potential may depend on the degree of electric percolation or the macroscopic geometric structure of the clusters of the conducting species.

We report here the derivation of the Nernst equation including percolation. The degree of percolation may vary with film thickness. Unfortunately, it is not easy to control film thickness while maintaining film uniformity because polyaniline aggregates yield patched films. We instead use suspended PANI-latex particles with various diameters.

2. Derivation of the Nernst equations

We consider the electrochemical reaction associated with the *n*-electron transfer between leucoemeraldine R and emeraldine O. It is known that one or two electrons are exchanged among four neighboring aniline units [2]. The electrochemical potential of R is written as

$$\overline{\mu}_{\mathrm{R}} = \mu_{\mathrm{R}}^{\circ} + RT \ln a_{\mathrm{R}} + z_{\mathrm{R}} F \phi_{\mathrm{S}} \qquad (1)$$

where a is the activity, z is the redox charge, and the subscript designates the species (R). Because R is the electrically insulating species in the solution phase, it has the inner potential of the solution, ϕ_{S}. However, the electrically conducting species O has the inner potential either of the electrode or of the solution, depending on whether it is electrically percolated with the electrode. The electrochemical potential of O can take either of the following two

forms:

$\overline{\mu}_{OS} = \mu_O^\circ + RT \ln a_{OS} + z_O F \phi_S$ (without electric connection to the electrode) (2)

$\overline{\mu}_{OE} = \mu_O^\circ + RT \ln a_{OE} + z_O F \phi_E$ (with electric connection to the electrode) (3)

where ϕ_E is the inner potential of the electrode. The electrochemical potential of the exchanged electron is given by

$\overline{\mu}_e = \mu_e^\circ - F\phi_E$ (4)

When the species O has ϕ_S, the equilibrium condition is given by

$\overline{\mu}_R = \overline{\mu}_{OS} + n\overline{\mu}_e$

Inserting Eq.(1), (2) and (4) into the above equation and using charge balance, $z_O - z_R = n$, we have

$E = E^\circ + (RT/nF)\ln(a_{OS}/a_R)$ (5)

where we expressed $\phi_E - \phi_S = E$ and $(n\mu_e^o + \mu_O^o - \mu_R^o)/nF = E^o$. This is the conventional Nernst equation.

When species O takes ϕ_E, on the other hand, the equilibrium condition is given by

$\overline{\mu}_R = \overline{\mu}_{OE} + n\overline{\mu}_e$

Inserting Eq.(1), (3) and (4) into the above equation yields

$-z_R E = E^\circ + (RT/F)\ln(a_{OE}/a_R)$ (6)

Because z_R is zero in the molecular form of leucoemeraldine, the equilibrium potential cannot be determined by the ratio of a_{OE}/a_R. In other words, the oxidized species percolated to the electrode does not participate in the determination of the electrode potential.

We replace the activities by the amounts adsorbed on the electrode through $a_R \rightarrow \Gamma_R$, $a_{OS} \rightarrow \Gamma_{OS}$, $a_{OE} \rightarrow \Gamma_{OE}$. The amount of the oxidized species, Γ_O, is given by $\Gamma_{OS} + \Gamma_{OE}$. Let the fraction of the unpercolated oxidized species be defined as

$\beta = \Gamma_{OS}/\Gamma_O$ (7)

Eq. (5) is rewritten as

$E = E^\circ + (RT/nF)\ln\beta + (RT/nF)\ln(\Gamma_O/\Gamma_R)$ (8)

The halfwave potential is given at $\Gamma_O = \Gamma_R$ by

$$E_{1/2} = E^{\circ} + (RT/nF)\ln\beta \qquad (9)$$

This potential varies with β-values, which may depend generally on the macroscopic structure of the film and specifically on film thickness, as well as exchange between O_E and O_S by thermal fluctuation and conversion rates of cyclic voltammetry.

When the film is so thin that O_S is not distinguished from O_E, values of $E_{1/2}$ may be independent of film thickness or electrolysis conditions. Equations (8) and (9) are interesting for thick films in which the local distribution of O_E and O_S do not vary during a voltammetric period. In other words, β can be evaluated in macroscopically thick films. If a small amount of the percolated species is localized only near the electrode surface, then the value of β is close to unity because $\Gamma_{OE} << \Gamma_O$ and $\Gamma_{OS} \approx \Gamma_O$. In this case, $E_{1/2}$ is close to E^o. This distribution may occur in the fast oxidation conditions. In contrast, the opposite distribution, $\Gamma_{OS} << \Gamma_O$ and $\Gamma_{OE} \approx \Gamma_O$, may be realized by a fast half-reduction in which O_E is left behind. Then, β is small, and $E_{1/2}$ is shifted negatively from E^o.

3. Experimental

Electropolymerized PANI films were synthesized by scanning the voltage once from 0.0 to 0.83 V vs. Ag|AgCl at 0.5 mV s^{-1} at the platinum disk electrode in 0.5 M aniline + 1 M sulfuric acid at 0^{o}C. This scan rate empirically provided nondestructive, smooth films. The thickness of the films was read from their cross sections obtained with an optical microscope, VH-5000 (Keyence, Osaka). The read thickness was associated with the charge of the background-subtracted charge density through the relation 0.075 μC mm^{-2} ↔ 1 μm. The background subtraction technique has been described previously [29]. Voltammetry was primarily done in 1.0 M sulfuric solution using platinum disk electrodes (0.5 mm or 1.6 mm in diameter), an Ag|AgCl reference electrode, and a Pt coil counter electrode with a Compactstat potentiostat (Ivium, Netherlands).

PANI latex suspensions were synthesized by coating polystyrene latex with PANI films

using a previously described method [30]. The size was controlled with polystyrene latex. The size and the amount of PANI per particle are listed in Table 1. Radii, *r*, of the latex particles were evaluated by a light scattering instrument (Malvern Zetasizer Nano-ZS, UK), SEM (Hitachi, S-2600H) and a video microscope VMS-1900 (Scalar). The amount ratio of PANI to core polystyrene was determined by dissolving the core-polystyrene of the latex to tetrahydrofuran and weighing the solvent-extracted PANI. Then the number of PANI units per particle, *m*, was calculated. The number concentration of the PANI particle was determined by removing salt with centrifugation and by weighing the dried latex.

Viscosity of the suspensions was varied by mixing the latex suspensions with glycerol (Wako) at various ratios, and was evaluated with Ostwald viscometer. The absolute value of the viscosity of glycerol was determined by means of a rotational viscometer, Visco (Viscoteck, Tokyo), at room temperature.

4. Results and Discussion

The PANI suspension was initially in the emeraldine state, judging from the color of the PANI and the 0.5 V open circuit potential, which is in the potential domain of the emeraldine form. It was not aggregated after standing for one month. The dried suspensions showed uniform size distributions of a regular arrangement of spherical particles [30]. The suspension in acid solution turned from dark green to dark blue when it was transferred into neutral solution or basic solutions. Figure 1(b) shows the voltammogram of PANI-suspended sulfuric acid at the Pt electrode, together with that (a) in sulfuric acid at the PANI-coated electrode. The PANI suspension only exhibited a cathodic wave, whereas the PANI-coated electrode showed an anodic sharp peak as well. The absence of any oxidation wave for the suspension has been interpreted as a combination of the electric percolation and the propagation of the conducting zone as follow [30]; the conducting particle is reduced rapidly to the insulating species by the collision with the electrode, keeping a constant potential at

the electrode and the conducting species, whereas the oxidation is controlled by the propagation speed of the conducting zone with slow kinetics. The other feature of the voltammogram of the PANI suspension is the potential shift of the reduction wave in the positive direction from that of the PANI film. The potential shift is our concern in this report.

We examined the rate-determining step of the reduction peak current of the suspension. The peak currents divided by the PANI concentrations, mc, (m: the number of PANI units per particle, c: the concentration of particles) were proportional to the square-roots of the scan rates, v, for $0.01 < v < 0.15$ V s^{-1}, as is shown in Fig. 2, irrespective of size of the latex. Therefore, they should be controlled by the diffusion of the suspended PANI particles to the electrode. The decrease in the slopes with an increase in radii is ascribed to the decrease in the diffusion coefficient of latex, D, through the Stokes-Einstein equation. The voltammetric peak current for multiple electron transfer reactions is expressed by [31]

$$I_p = 0.446FAmc(DvF/RT)^{1/2} \quad (10)$$

where A is the area of the electrode. From the proportional variation of I_p to c and $v^{1/2}$, values of D were evaluated and are listed in Table 1. They are close to the values calculated from the radii of the latex by the Stokes-Einstein equation.

The reduction peak potential, E_{pR}, shifted in the negative direction with an increase in the latex diameter and was slightly dependent on the scan rates, as shown in Fig. 3. In other words, large particles are more difficult to reduce than smaller particles. The shift was pronounced for small particles ($2r < 1$ μm), but it did not vary for large diameters of $2r > 3$ μm. A value of E_{pR} for a particle with a diameter of only a few nanometers particle might be interesting because it would approach the size-independent value, E^o. Unfortunately, we were not able to synthesize particles smaller than 0.2 μm in diameter because of difficulty in the sedimentation by centrifugation at the purification step. We estimated the value of E_{pR} for the smallest particle by extrapolating the diameter to zero, as shown in Fig. 3. We obtained $(E_{pR})_{r\to 0} = 0.31$ V vs. Ag|AgCl. Because the configuration and the tacticity of the synthesized PANI are independent of particle size, the size dependence of E_{pR} may be ascribed to

macroscopic structural features such as the polymerization degree, micellization effects by the surfactant (PVP), partial redox reactions for dispersed latex [32-34], rotational diffusion [35] and the percolation effect [25,26,36]. The last feature is likely to occur in PANI with a scale of few microns because the electric percolation is a long distance interaction [37].

Now, we discuss the variation of Fig. 3 in the light of the percolation by using Eq. (8) and (9). According to the theory of diffusion-controlled voltammograms [38], the reduction peak current appears at -28.5/n mV + E^{o} at 25 ^{o}C for common values of diffusion coefficients of O and R. Eq. (8) is then rewritten as $E_{pR} = E^{o} + (RT/nF) \ln \beta$ -28.5/n mV. The subtraction of E_{pR} from $(E_{pR})_{r\to 0} = E^{o}$ -28.5/n mV yields

$$(1/n)\ln\beta = \left(E_{pR} - \left(E_{pR}\right)_{r\to 0}\right) F/RT \qquad (11)$$

We evaluated (1/n) log(β) from E_{pR} and $(E_{pR})_{r\to 0}$ for several values of the PANI particle radii, and plotted them against log r in Fig. 4. All points fell on a line that was empirically subject to

$$(1/n)\log\beta = -3.3\log(r/\mu\mathrm{m}) - 3.3 \qquad (12)$$

The value of n is reported to range from 0.2 to 0.4, which has been explained by a redox reaction in which one unit of the four aniline moieties participates in the conversion of emeraldine to leucoemeraldine [39]. In this case, the power, -3.3n, ranges from -0.7 to -1.2, and is close to -1. Consequently, we have for a constant k

$$\beta \equiv \Gamma_{OS}/\Gamma_{O} = k/r \qquad (13)$$

This result allows us to propose a reaction model for the polystyrene-PANI particle. When a fully conducting particle toward the electrode collides with the electrode at the cathodic potential, it possesses the same potential as the electrode because of the electric contact. The reduction begins at the whole PANI domain covering the polystyrene sphere and proceeds rapidly [8,23, 26] until the oxidized concentration reaches the threshold value, Γ_{O}^{t}, for the electric percolation, illustrated in Fig. 5(A). With the progress in the reduction by dispersion of conducting species ($\Gamma_{O} < \Gamma_{O}^{t}$), the oxidized species loses electric percolation to

the electrode because of the cutoff in electric path. The oxidized species is left behind at the top part of the sphere, keeping the value of Γ_O^t (in Fig. 5(B)), as demonstrated in photographs and in the simulation [36]. Let the height of the domain with Γ_O^t from the electrode be h, which is along the surface of the sphere at the angle, θ. Because $h = r(1 - \cos\theta)$, the volume of the PANI δ in thickness included in θ is expressed by

$$V(\theta) = \delta\int_0^\theta 2\pi r(\sin\phi)r\mathrm{d}\phi = 2\pi\delta r^2(1-\cos\theta) = 2\pi\delta rh$$

Using the expression for the total volume of the PANI on the surface, $V(\pi) = 4\pi\delta r^2$, the ratio of the two volumes is given by $V(\theta)/V(\pi) = h/2r$. The volume ratio is equivalent to the empirical equation (13). We have successfully interpreted the empirical linearity in Fig. (4) in terms of the geometrical limitation of the reduction, i.e.,

$$\beta \equiv \Gamma_{OS}/\Gamma_O = h / 2r \qquad (14)$$

Using $3.3n = 1$, combination of Eq. (12) with Eq. (14) yields $\beta = (10\ r\ /\ \mu\mathrm{m})^{-1} = h / 2r$. We then have ca. $h = 0.2$ μm. This is close to the smallest particle (Table 1).

The height h may depend on the reduction period of the particle remaining on the electrode. Because viscous solutions decrease diffusion coefficients, they are expected to increase the staying period and shift the peak potential in the negative direction. Viscosity was varied by addition of glycerol to the suspensions, keeping the acidity and the concentration of the latex constant. Figure 6 shows variations of E_{pR} with the viscosity, η, at different scan rates. As predicted, E_{pR} decreased with an increase in viscosity, almost independent of the scan rates. Therefore, the potential shift is caused not only by the thermodynamic effect in Eq. (8) but also by the dynamic effect under practical conditions.

We used the electrochemically polymerized film to vary the cathodic peak potentials with scan rates. The anodic and cathodic peak currents were proportional to the scan rate, as predicted from surface waves. The anodic peak potential increased with v owing to solution resistance, as shown in Fig. 7(A). The cathodic peak potential also shifted (Fig. 7(B)) in the positive direction or $v < 2$ V s^{-1}. The direction of the shift is opposite to that of the effects of

IR-drop, electrode kinetics or chemical complications. The shift was more remarkable for thicker films. Chemical complications usually cause a potential shift. This shift would be observed with CV scan rate dependence more strongly than film thickness dependence. We observed negligibly small variations in the peak potentials with scan rates for thin films (Fig. 1(a)). Therefore, participation in chemical complications is neglected in the present experiments.

We evaluated β from the values of E_{pR} in Fig. 7 by using Eq. (11) at $3.3n = 1$. The values of β (= Γ_{OS}/Γ_{O}) were as small as 0.1, indicating that majority of the oxidized species should be percolated to the electrode. This prediction is illustrated in Fig. 5(c), where the film is much thicker than h. They increased linearly with v for $v < 1$ V s^{-1}, as is shown in Fig. 8. Two reasons for the increase can be considered: a decrease in the reduction potential at the reduction surface on O_E and a delay in mass transport of hydrogen ions into the film.

5. Conclusion

The model for the derivation of the Nernst equation is an inhomogeneous distribution of oxidized percolated, oxidized nonpercolated, and reduced PANI molecules normal to the electrode. It is not valid for monolayer films. The conducting species (emeraldine) percolated to the electrode does not contribute to the determination of the equilibrium potential because it takes the inner potential of the electrode and loses the redox information. Consequently, the electrode potential is determined by the ratio of the amount of the nonpercolated oxidized species to that of the reduced species. We defined partition of the nonpercolated oxidized species, β, as a measure of the amount of the potential-determined species. The potential is shifted in the positive direction by (RT/F) ln β with an increase in the amount of the percolated species. Because thick films have large values of the percolated species, or small values of β, the redox potential should be shifted in the positive direction.

To demonstrate this prediction experimentally, we used suspended polyaniline latex

particles with various radii. The larger the latex radii, the more positive the cathodic peak potentials of the voltammetric currents. The peak potential without the percolation effect was estimated to be 0.31 V vs. Ag|AgCl from extrapolation to zero radii. A geometrical model for the percolation domain in the sphere was proposed in which a given portion of the particle was electrically connected to the electrode irrespective of particle size. The peak potential shift was also observed in the variation of the viscosity, or the diffusion coefficient. One extreme, large particles in high viscosity, corresponds to a polyaniline film. The peak potential shift was found in the variation of scan rates in electropolymerized polyaniline-coated electrodes.

Figure Captions

Figure 1. Cyclic voltammograms of (a) the PANI-coated Pt electrode in 0.5 M sulfuric acid and (b) of the PANI-latex suspension at v = 0.1 V s^{-1} at the first scan. The average thickness of the film was 0.3 μm, evaluated from the charge of the CV.

Figure 2. Variation of the cathodic peak currents with the square-roots of the scan rates for PANI particles with (a) 0.40, (b) 0.89, (c), 3.90 and (d) 7.50 μm in diameter.

Figure 3. Dependence of the cathodic peak potential, E_{pR}, in the PANI-latex suspension on the diameters of the latex particles. Voltammograms were obtained at v = (full circles) 0.01, (triangles) 0.05 and (open circles) 0.1 V s^{-1} in the solution of 5 g dm^{-3} latex suspension.

Figure 4. Dependence of β evaluated from Eq. (11) on r. The marks are the same as in Fig. 3.

Figure 5. A model of the redox reaction of the PANI-coated latex particle which comes in contact with the electrode when the reduction proceeds from the threshold concentration (A) to the less concentration (B). The black domain represents the conducting species with the percolation threshold concentration, Γ_O^t, whereas the grey domain does the conducting species with concentration less than Γ_O^t. A film (C) behaves like the particle.

Figure 6. Variation of E_{pR} with viscosity, η, of the PANI suspensions at v = (open circles) 0.01, (triangles) 0.05 and (full circles) 0.1 V s^{-1}.

Figure 7. Variations of the (A) anodic and (B) cathodic peak potentials with the scan rates for voltammograms at the electrochemically polymerized PANI films (filled) 1.5 μm and (open) 15 μm thick in 1 M H_2SO_4 acid.

Figure 8. Dependence of β calculated from E_{pR} of the electropolymerized films through Eq. (11) on $v^{1/2}$.

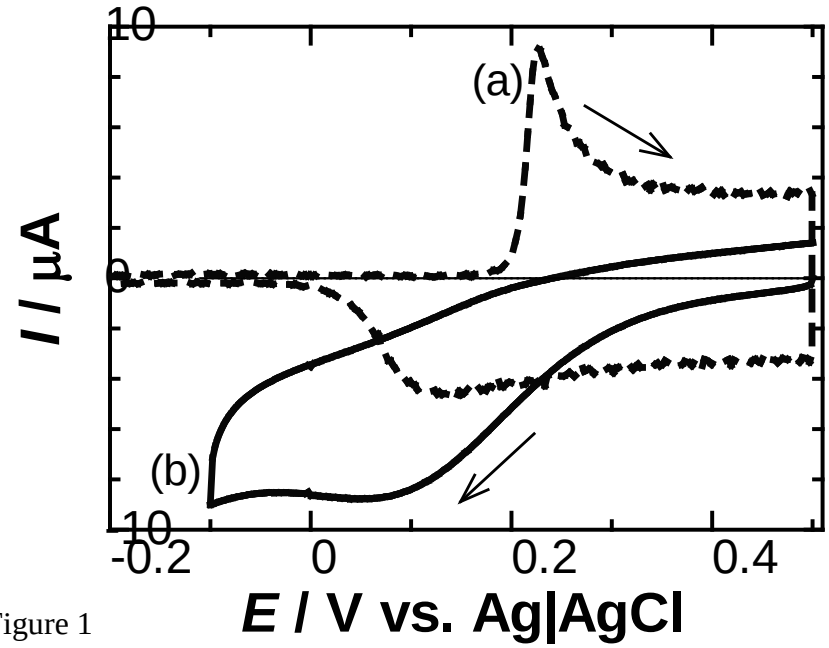

Figure 1

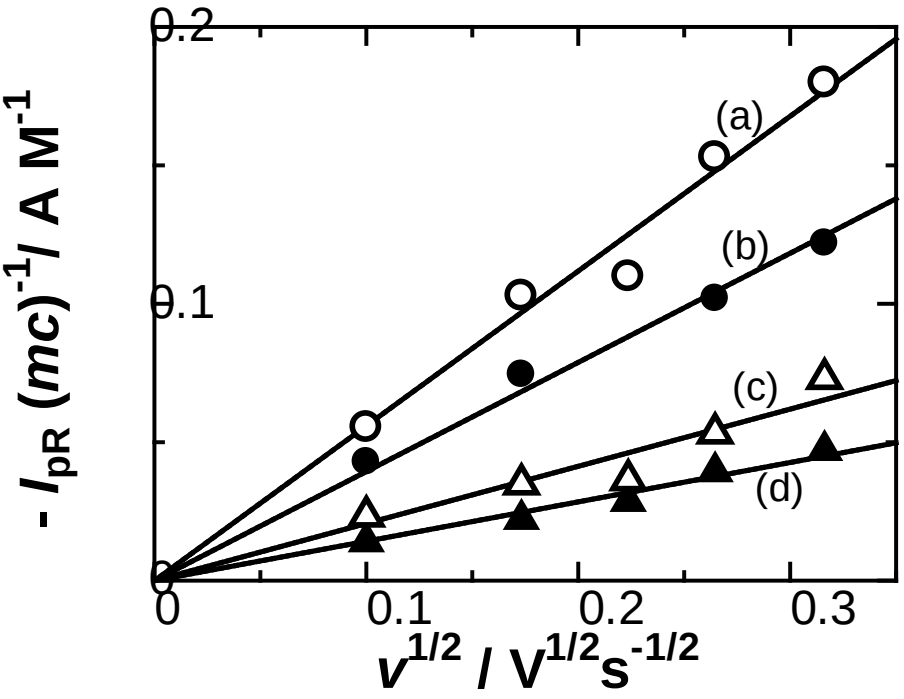

Figure 2

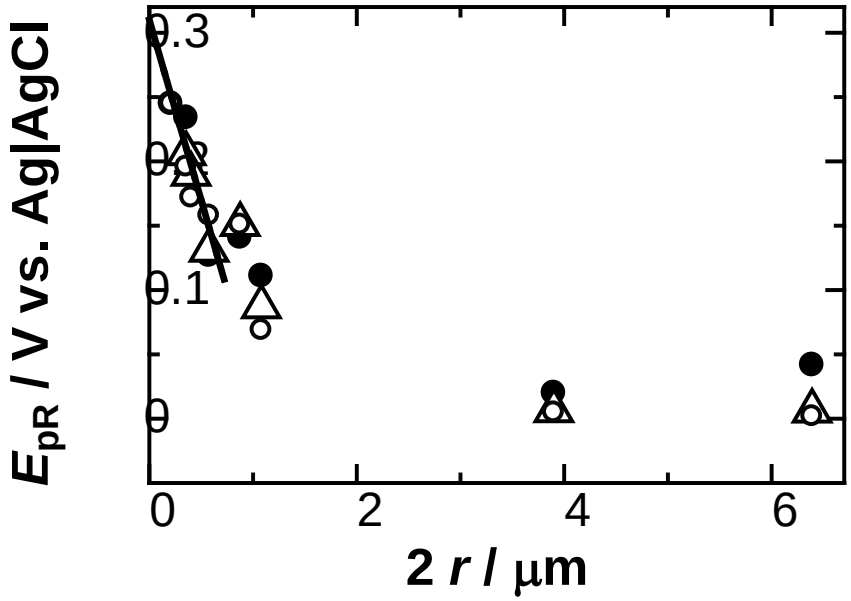

Figure 3

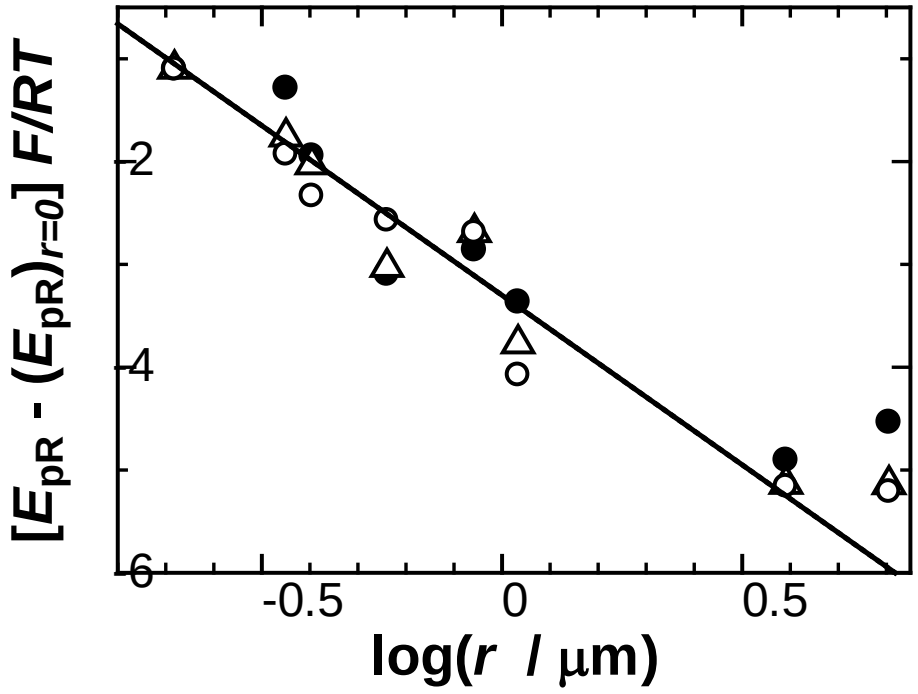

Figure 4

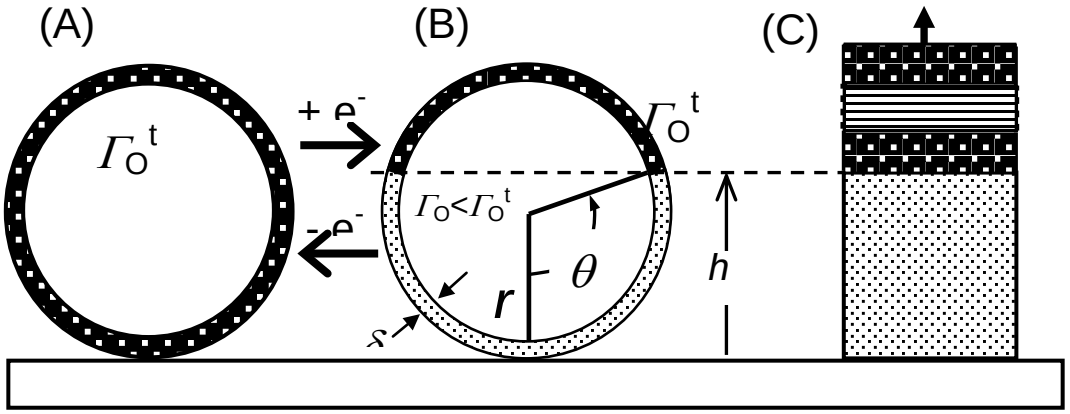

Figure 5

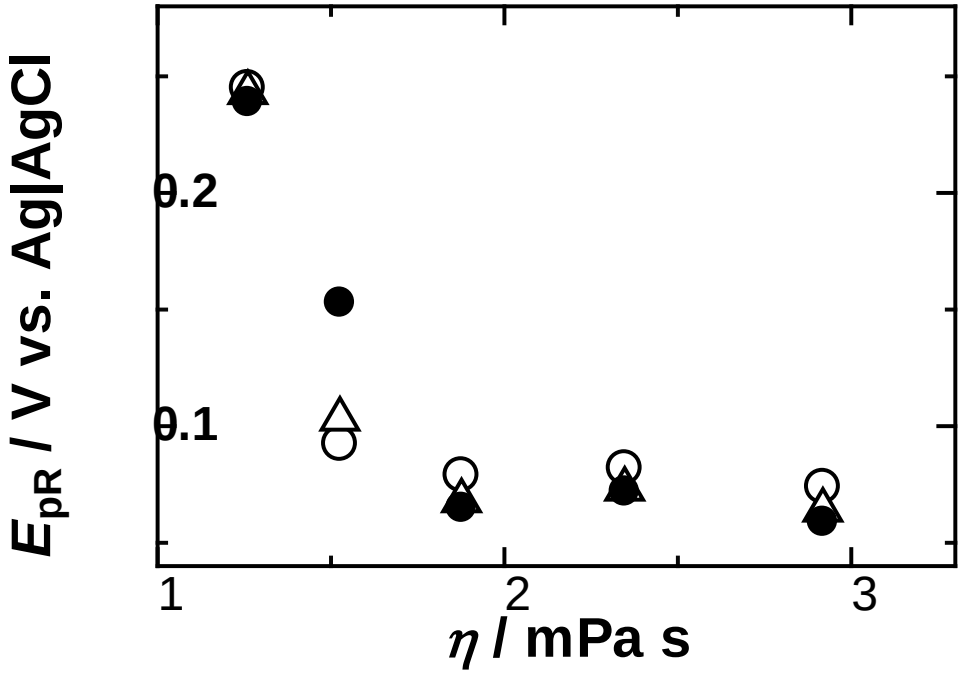

Figure 6

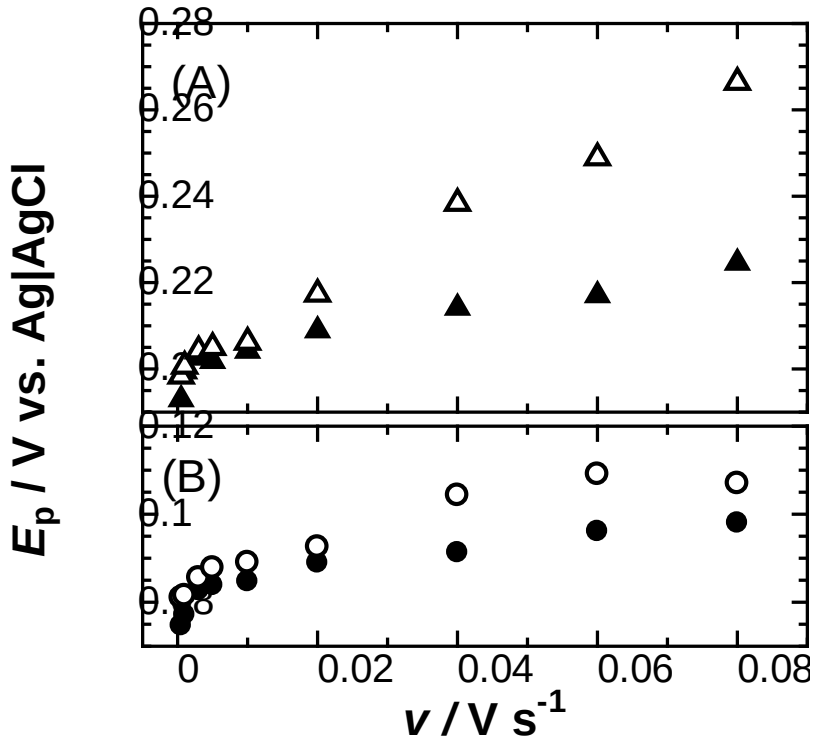

Figure 7

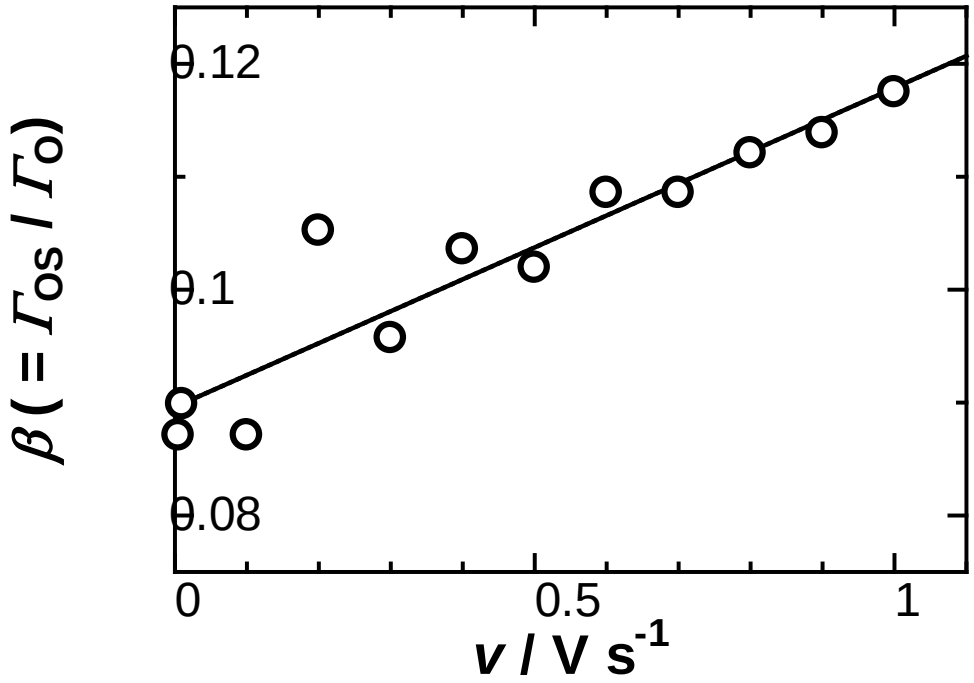

Figure 8

Table 1. Amount of PANI loaded on one particle

	$2r$ / μm	W_{PS}/W_{PA} a)	δ / nm b)	m c)	$D \times 10^9$/ $cm^2\ s^{-1}$ d)	$D \times 10^9$/ $cm^2\ s^{-1}$ e)
1)	0.20	4.35	5	3.2×10^6	24.	18
2)	0.40	9.38	5	5.0×10^7	12.	13
3)	0.58	6.47	10	7.6×10^8	8.5	7.5
4)	0.89	10.7	9	8.4×10^8	5.6	3.1
5)	1.08	4.65	25	2.3×10^9	4.5	3.2
6)	3.90	3.26	125	5.6×10^{10}	1.3	0.88
7)	6.41	6.15	116	3.0×10^{11}	0.76	0.53
8)	7.50	3.76	212	6.6×10^{11}	0.65	0.45

a) weight ratio of polystyrene to PANI, b) thickness of PANI film calculated from the weight ratio and the radii, c) the number of redox site of PANI per particle, d) diffusion coefficient calculated from the Stokes-Einstein equation in water, e) diffusion coefficient obtained from the peak current and Eq.(11).

References

[1] G. P. Evans, Advances in Electrochemical Science and Engineering, Vol. 1, edited by H. Gerischer and C. W. Tobias, VCH Publishers Inc., New York, 1990.

[2] A.J. Epstein, J.M. Ginder, F. Zuo, R.W. Bigelow, H.-S. Woo, D.B. Tanner, A.F. Richter, R, W.-S. Huang, A.G. MacDiarmid, Synth. Met. 18 (1987) 303.

[3] T. Kobayashi, H. Yoneyama, H. Tamura, J. Electroanal. Chem. 177 (1984) 293.

[4] K. Aoki, S. Tano, Electrochim. Acta, 50 (2005) 1491.

[5] R.L. Hand, R.F. Nelson, J. Am. Chem. Soc. 96 (1974) 850.

[6] D.E. Stilwell, S.M. Park, J. Electrochem. Soc. 135 (1988) 2491.

[7] S. W. Feldberg, I. Rubinstein, J. Electroanal. Chem. 240 (1988) 1.

[8] J. Cao, K. Aoki, Electrochim. Acta 41 (1996) 1787.

[9] T. F. Trero, H. Grande, J. Rodriguez, Electrochim. Acta 41 (1996) 1863.

[10] A. R. Hillman, S. Bruckenstein, J. Chem. Soc. Faraday Trans. 89 (1993) 339

[11] Q. Pei, O. Inganas, J. Phys. Chem. 97 (1993) 6034.

[12] M. Grzeszczuk, P. Poks, Synth. Met. 98 (1998) 25.

[13] E. F. Bowden, M. F. Dautartas, J. F. Evans, J. Electroanal. Chem. 219 (1987) 49.

[14] A. G. MacDarmid, J. C. Chaing, A. F. Richer, A, J. Esptein, Synth. Met. 18 (1986) 285.

[15] T. Kobayashi, H. Yoneyama, H. Tamura, J. Electroanal. Chem. 177 (1984) 281.

[16] B. J. Feldman, P. Burgmayer, R. W. Murray, J. Am. Chem. Soc. 107 (1985) 872.

[17] W. W. Focke, G. E. Wnek, J. Electroanal. Chem. 256 (1988) 343.

[18] C. Barbero, M. C. Miras, O. Haas, R. Kotz, J. Electrochem. Soc. 138 (1991) 669.

[19] G. Horanyi, G. Inzelt, Electrochim. Acta 33 (1988) 947.

[20] A. R. Hillman, M. J. Swann, S. Bruckenstein, J. Phys. Chem. 95 (1991) 3271.

[21] M. A. Mohamoud, A. R. Hillman, Electrochim. Acta, 53 (2007) 1206.

[22] K. Xu, L. Zhu, Y. Wu, H. Tang, Electrochim. Acta, 51 (2006) 3986.

[23] K. Aoki, T. Edo, J. Cao, Electrochim. Acta, 43 (1997) 285.

[24] K. Aoki, T. Aramoto, Y. Hoshino, J. Electroanal. Chem., 340 (1992) 127.

[25] K.Aoki, J. Cao, Y. Hoshino, Electrochim. Acta, 38 (1993) 1711.

[26] K. Aoki, Cao, Y. Hoshino, Electrochim. Acta, 39 (1994) 2291.

[27] J. C. Chiang, A. G. MacDiarmid, Synth. Met. 13 (1986) 193.

[28] K. Aoki, Electrochem. Comm. 2 (2000) 94.

[29] Y. Tezuka, K. Aoki, K. Shinozaki, Synth. Metals, 30 (1989) 369.

[30] H. Chen, J. Chen, K. Aoki, T. Nishiumi, Electrochim. Acta, 53 (2008) 7100.

[31] K. Aoki, Electroanalysis, 17 (2005) 1379.

[32] C. Xu, K. Aoki, Langmuir 20 (2004) 10194.

[33] L. Han, J. Chen, K. Aoki, J. Electroanal. Chem. 602 (2007) 123.

[34] J. Chen, K. Aoki, T. Nishiumi, T. Li, Langmuir, 22 (2006) 10510.

[35] K. Aoki, Electrochim. Acta, 51 (2006) 6012.

[36] K. Aoki, Y. Teragishi, J. Electroanal. Chem. 441 (1998) 25.

[37] D. Stauffer, A. Aharony, Introduction to Percolation Theory, 2nd ed., Taylor & Francis, 1992, London, pp. 1-13.

[38] R. S. Nicholson, I. Shain, Anal. Chem. 36 (1064) 706.

[39] W. S. Huang, B. D. Humphrey, A. G. MacDiarmid, J. Chem. Soc. Faraday Trans. 1, 82 (1986) 2385.